THE DEPENDANCE OF RADAR BACKSCATTER FROM DOMINANT WAVELENGTH WATER WAVES

Benjamin E. Barrowes
Brigham Young University, MERS Laboratory
459 CB, Provo, UT 84602
801-378-4884, FAX: 801-378-6586, barroweb@et.byu.edu

Abstract—Radar backscatter characteristics of sea surfaces depend on many difficult to describe parameters. These parameters include wind speed, incidence angle of the scatterometer, wind direction, frequency used, height of the instrument above the water, footprint size, and the underlying tilt of the waves themselves among others. An ultrawideband scatterometer named YSCAT94 gathered six months of data while deployed at the Canada Center for Inland Waters (CCIW) research platform in Lake Ontario. The backscatter distributions for small footprint scatterometers like YSCAT94 depend on the dominant wavelength of the sea. This paper gives a brief overview of the YSCAT94 instrument and then details the probability model which relates dominant wave slope to backscatter returns. The method used to calculate the dominant wave slope from YSCAT94 data is then presented followed by a conclusion and future directions.

Introduction

Microwave remote sensing of the air-sea interface has many important applications such as weather forecasting and microwave anemometry. Potentially, satellites could offer daily global wind estimates over Earth's oceans. Though various experiments nave been conducted for the purpose of furthering our understanding of the air-sea interface, there was a noticeable lack of a single cohesive data set which included varied conditions and parameters at a single site.

YSCAT94 was constructed at Brigham Young University by members of the MERS (Microwave Earth Remote Sensing) laboratory to operate over a range of frequencies (2-18GHz), incidence angles (0° (nadir) to 60°), and azimuth angles remotely and continuously. It was deployed for a period of six months from June to November at the CCIW site on Lake Ontario. YSCAT94 was designed to operate under varying environmental conditions using only a modem hookup for maintenance. Vital data such as backscatter strength, Doppler shift, and Doppler centroid were gathered. With this data, the air-sea interface could be studied in greater detail than before. Table 1 presents some of YSCAT94's RF parameters. The antenna beamwidth was kept nearly constant in order to achieve the same footprint size even while varying frequency.

Interpreting YSCAT94's unique data set and eventually applying the results to spaceborn scatterometry experiments depends on our understanding of the scattering mechanisms of the air-sea interface. For large footprint scatterometers, for example the NASA scatterometer (NSCAT), whose footprint size is many times larger than the correlation length of the sea surface, the backscatter is well modeled by a normal distribution as predicted by the central limit theorem. However, the backscatter distribution for small footprint scatterometers is still the subject of some debate. Various distributions such as the Weibull and the Rayleigh have been suggested, but more recent analysis by Gotwols and Thompson [1994] has given theoretical backing to the lognormal distribution. In an attempt to verify the validity of this distribution, the dominant wave slope was calculated from YSCAT94 data. The compound probability model, which relates dominant wave slope and backscatter return strength, serves as the link between the dominant wave slope and the backscatter distribution.

Compound Probability Model

The most common model for sea scattered radar return at moderate incidence angles is the composite model. This model assumes that the sea surface is composed of small patches. Each of these patches

Center Frequency	2-18 GHz
Peak Output Power	23 dBm
Transmit Polarization	V or H
Two-Way Antenna Beam width	$5-10°$
Receive Polarization	H and V
Polarization Isolation	15-20 dB
LO-IF	166 MHz
Dynamic Range	50-110 dB
Baseband Signal Bandwidth	900 Hz

Table 1: YSCAT94 RF System Parameters

has a cross section given by small perturbation theory (SPT) as,

$$\sigma_o = 16\pi k_m^4 |g_{ii}(\theta_i)|^2 \Psi(2k_m \sin\theta_i, 0) \quad (1)$$

where σ_o is the radar cross section, θ_i is the incidence angle, $g_{ii}(\theta_i)$ is a polarization dependant reflection coefficient with ii being hh or vv, k_m is the microwave wavenumber ($\omega\sqrt{\mu\epsilon}$ or $\frac{2\pi}{\lambda}$), and Ψ is the wave height spectral density [Reed, 1995].

These patches of relatively small waves, on the order of centimeters, are tilted by larger waves typically on the order on meters. Consequently, the radar backscatter distribution depends on the distribution (or tilt) of the larger waves present. One way this slope distribution can be described is by finding the dominant wavelength, or the water wave with the most energy. Finding this dominant wavelength in order to characterize the radar backscatter distribution will be the focus of section three. First, however, we'll follow the development of Gotwols and Thompson [Gotwols and Thompson, 1994] for finding a backscatter distribution model description with which we can compare our data.

The compound probability model, originally proposed by Valenzuela and Laing [1971], considers the aforementioned two scales of waves separately. Radar backscatter characteristics of the sea surface rely heavily on waves on the order or smaller than the radar footprint and on the underlying tilt imposed from waves with wavelengths much larger than the radar footprint. For the former case σ_o is considered constant but the amplitude of the return is allowed to vary yielding the conditional probability $p(a|\sigma_o)$. For the latter case, due to the relatively large scale of the wave, σ_o is allowed to vary with probability $p(\sigma_o)$. Thus the total distribution may be expressed as

$$p(\sigma_o) = \int p(a|\sigma_o)p(\sigma_o)ds. \quad (2)$$

The probability of measuring a given backscatter power a can be calculated by considering distributions on the orders of both scales. $p(a|\sigma_o)$ is generally considered to be Rayleigh distributed. The distribution of $p(\sigma_o)$ is the focus of the next section.

Once these two distributions are known, a form for $p(\sigma_o)$ can be calculated by Eq. (2) and compared with empirical data from an instrument such as YSCAT94.

Distribution of $p(\sigma_o)$

Referring back to Eq. (1), in order to completely determine σ_o we must find expressions for the reflection coefficients g_{ii} and the wave height spectral density $\Psi(2k_m \sin\theta_i, 0)$. From Plant [Plant, 1986] we find the reflection coefficients to be,

$$|g_v(\theta_i)|^2 = \frac{\cos^4\theta_i(1+\sin^2\theta_i)^2}{(\cos\theta_i + 0.111)^4} \quad (3)$$

and

$$|g_h(\theta_i)|^2 = \frac{\cos^4\theta_i}{(0.111\cos\theta_i + 1)^4} \quad (4)$$

where θ_i is the incidence angle between the radar and the water surface.

Various wave height spectrums have been proposed and used [Phillips, 1985] [Durden and Vesecky, 1985] [Plant, 1986]. The wave height spectrum used in this paper was calculated from empirical data from in situ measurements at Lake Ontario by Donelan et al [Donelan, Hamilton, and Hui, 1985]. The frequency spectrum (related to the wave height spectrum) can be expressed as,

$$\Phi(\omega) = \alpha g^2 \frac{\omega^{-4}}{\omega_p} e^{-\frac{\omega_p}{\omega}} \gamma^\Gamma \quad (5)$$

$$\Gamma = e^{-(\omega-\omega_p)^2/2\sigma^2\omega_p^2} \quad (6)$$

where ω_p is the spectral peak, α is the equilibrium range parameter, γ is the peak enhancement factor, and σ is the peak width factor. The parameter α is given by

$$\alpha = 0.006(U\cos\theta/c_p)^{0.55} \quad (7)$$

where U is the wind speed and c_p is the phase velocity of the peak frequency wave. The peak enhancement factor (γ) is given by:

$$\gamma = 1.7 + 6\ln(U/c_p). \quad (8)$$

The peak width parameter is given by

$$\sigma = 0.08\left(1 + \frac{4}{(U\cos\theta/c_p)^3}\right) \quad (9)$$

and the ratio $U\cos/c_p$ is given by:

$$U\cos\theta/c_p = 11.6\tilde{x}^{-0.23} \quad (10)$$

where $\tilde{x}$ is the non-dimensional fetch.

The fetch (the distance over which the wind blows over the water) is approximated to be 6km at the CCIW site [Reed, 1995].

Using this spectrum and the aforementioned reflection coefficients, σ_o versus incidence angle was plotted and is shown in Figure 1.

Figure 1 relates σ_o to θ_i, but another representation is to plot σ_o versus dominant wave slope instead.

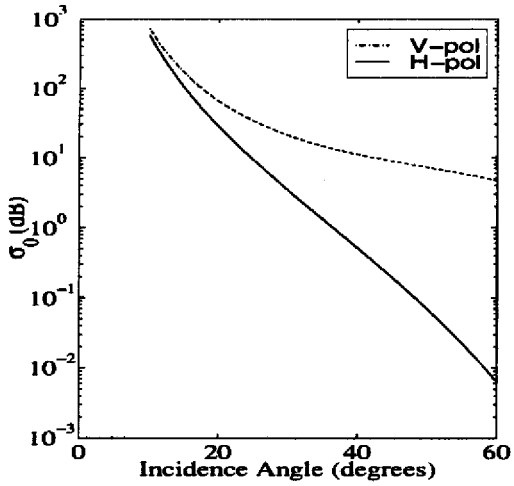

Figure 1: Incidence angle versus σ_o plotted from the Donelan spectrum. 14GHz, wind speed 8m/s, fetch is 9km.

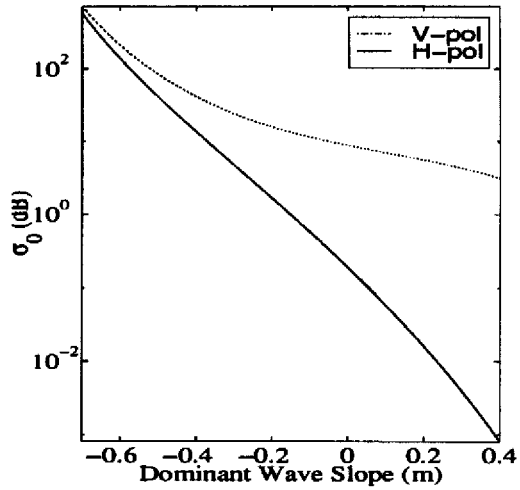

Figure 3: Dominant wave slope versus σ_o plotted from the Donelan spectrum. 14GHz, wind speed 8m/s, fetch is 9km.

The dominant wave slope is related to the local incidence angle (θ_i between the incident radar wave and the mean plane of the water) and the nominal incidence angle (θ_o the angle between the incident radar wave and the tilted water surface) by the following equation,

$$\chi + \theta_i = \theta_o \tag{11}$$

and

$$\tan\chi = -s_x. \tag{12}$$

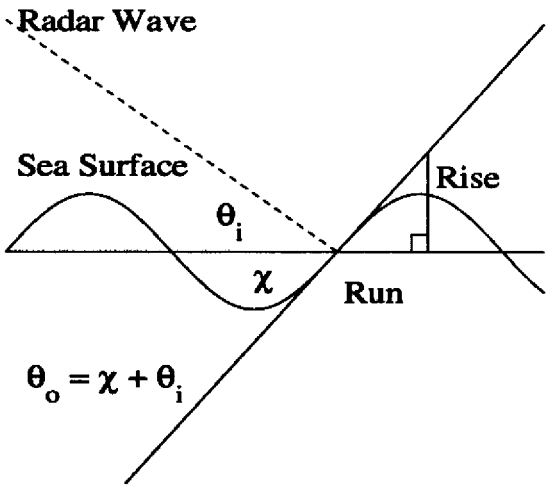

Figure 2: Relationship between χ , θ_i , and θ_0 . Dominant wavelength can be described by the "rise" over the "run".

This situation is shown in Figure 2.

In Figure 3 the radar cross section is plotted versus dominant wave slope.

Gotwols and Thompson [1994] noted the highly linear nature of the h-pol return and the quadratic nature of the V-pol return over mid-range incidence angles (20° - 50°). As a result, they proposed a quadratic model (in log space) for σ_o versus dominant wave slope,

$$\sigma_{op} = Ce^{a_1 s_x + a_2 s_x^2} \tag{13}$$

where p is either v or h.

This model for σ_{op} is justified by the close agreements of first and second order fits to σ_o versus dominant wave slope as can be seen from Figure 3. Now, using Eq. (13) we can find an expression for $p(\sigma_o)$ by the transformation law for probability density and assuming $p(s_x)$ is normally distributed with variance σ_x^2,

$$p(\sigma_o) = \frac{p(s_x)}{|d\sigma_o/ds_x|}. \tag{14}$$

Noting that

$$\begin{aligned} |d\sigma_o/ds_x| &= C(a_1 + 2a_2 s_x)e^{a_1 s_x + a_2 s_x^2} \\ &= (a_1 + 2a_2 s_x)\sigma_{ov} \end{aligned} \tag{15}$$

and

$$s_x = \frac{-a_1 \pm \sqrt{a_1^2 + 4a_2 ln(\frac{\sigma_{ov}}{C})}}{2a_2} \tag{16}$$

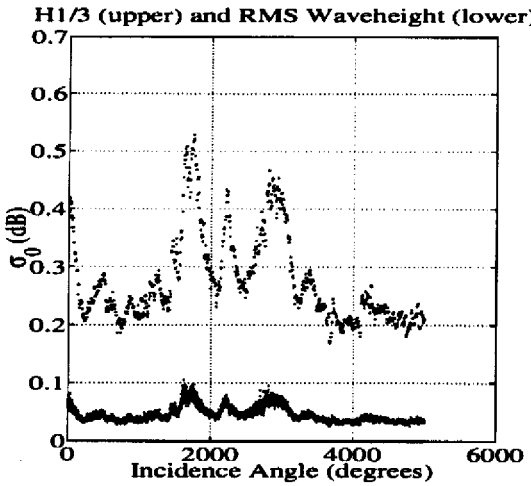

Figure 4: Comparison of $H\frac{1}{3}$ wave height (upper data) and RMS wave height (lower data). Similar trends can be seen indicating a strong correlation.

it can be shown that for h-pol (a_2=0),

$$p(\sigma_{oh}) = \frac{1}{a_1 \sigma_x \sigma_{oh} \sqrt{2\pi}} \exp\left(\frac{-(ln\sigma_{oh} - lnC)^2}{2a_1^2\sigma_x^2}\right) \quad (17)$$

and for vertical polarization,

$$p(\sigma_{ov}) = \frac{1}{(a_1 + 2a_2 s_x)\sigma_x \sigma_{ov} \sqrt{2\pi}} \exp\left(\frac{-(s_x)^2}{2\sigma_x^2}\right) \quad (18)$$

with s_x as defined by Eq. (16) and for the zero mean case. Eq. (17) is referred to as the lognormal distribution. This can serve as the distribution of the backscatter (σ_o) for a given slope distribution.

The next step is to calculate the dominant wave slope (s_x) for the period that YSCAT94 was in operation and use these values to experimentally verify the above model. In the process, the parameters a_1 and a_2 need to be calculated from the data.

Extracting the Dominant Wave Slope

The dominant wave slope, similar to other slopes, may be generally described by calculating the "rise" over the "run". In the case of sea or ocean waves, the "rise" is a parameter referred to as $H\frac{1}{3}$, and the "run" is the dominant wavelength (λ).

Calculating $H\frac{1}{3}$

The parameter $H\frac{1}{3}$ was first presented by Sverdrup and Munk [Sverdrup and Munk, 1947] as the average of the highest $\frac{1}{3}$ of the waves and is equal to approximately 4σ. $H\frac{1}{3}$ was calculated for the entire six months of YSCAT94 data. $H\frac{1}{3}$ should correlate closely with the RMS (root mean square) wave height. This was indeed the case as the same trends can be seen in Figure 4.

Calculating the Dominant Wavelength

During the period of May through November 1994 when YSCAT94 was in operation, Donelan et al of the CCIW monitored a wave staff array consisting of eight staves at the same location. These eight wave staves were designed to measure the height of the water surface at $\frac{1}{10}$ second intervals. Using this data, which overlapped YSCAT94's data, the frequency spectrum of the sea surface was calculated, and the dominant wavelength λ was calculated.

The sampling time of the wave staves was small enough to permit resolution of wavelengths smaller than the dominant wavelengths. According to the Nyquist criterion, with a sample rate of $\frac{1}{10}$ seconds, wavelengths with a period of $\frac{2}{10}$ seconds are resolvable. The wavelength and frequency of water waves are given by the dispersion relation for water:

$$\lambda = \frac{g}{2\pi f^2} \quad (19)$$

where λ is the wavelength, g is the acceleration of gravity, and f is the frequency of the wave. For period T= $\frac{1}{f} = \frac{2}{10}$ seconds, $\lambda \approx$ 6cm. In comparison, for the Lake Ontario site, dominant wave periods of up to 4 seconds ($\lambda \approx$ 25m) are common [Donelan, Hamilton, and Hui, 1985].

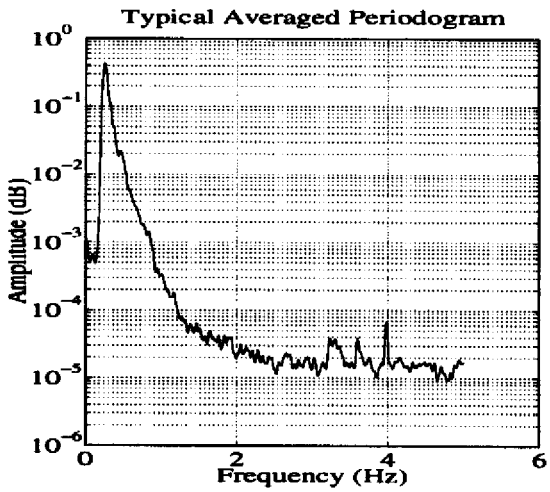

Figure 5: Typical power spectrum calculated from wave staff measurements at CCIW tower in Lake Ontario. Peak is at f=.26Hz, $\lambda \approx$ 23m.

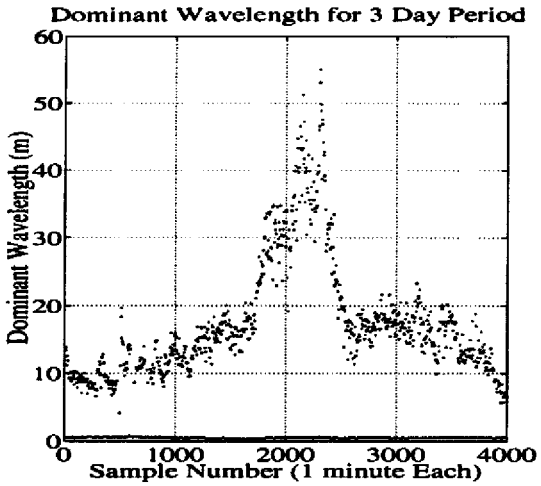

Figure 6: Dominant wavelength time series for a 3 day period. Calculated from YSCAT94 data.

YSCAT94 collected data for 17 minutes periods and performed maintenance tasks for three minutes leading to 20 minute data records. For each of the 17 minute periods, $H\frac{1}{3}$ and the dominant wavelength were calculated at four different points corresponding to about four minutes of data each. This length was chosen to allow the greatest resolution for each data record while still being long enough for >20 dominant waves in the data window of four minutes.

A windowed, detrended, averaged, periodogram method (Welch's) was chosen to calculate the power spectrum from which the dominant wavelength could be retrieved. The windowed, averaged, spectrum was then smoothed by averaging groups of four samples centered at each data point thus effectively eliminating much of the noise [see Figure 5.]

This spectrum corresponds to the frequency content of the sea waves during the data collection period. The typical k^{-4} falloff often associated with ocean wave spectra can be observed on the high frequency side of the main spike. The spectral peak of this time period occurs at a frequency of approximately .26Hz which corresponds to a dominant wavelength of approximately 23m. This is the point in the spectrum with the most energy and is thus called the dominant wavelength. A time series of dominant wavelengths calculated from almost nine hours of YSCAT94 data is shown in Figure 6.

Conclusion

The dominant wave slope of the sea surface was calculated from YSCAT94 data taken from six months of deployment at CCIW on Lake Ontario. The compound probability model which gives theoretical backing to the lognormal distribution was presented. Further work is needed in order to fully understand backscattered radar distributions. YSCAT94 data must be sorted into homogeneous sets of matching wind speed, incidence angle, azimuth angle, etc. and then fitted to the lognormal distribution. In the process, a_1 and a_2 will need to be calculated, analyzed, and compared to Gotwols and Thompson's model. It is hoped that using YSCAT94's unique data set, a better understanding of the scattering of radar waves of small footprint radars from the sea surface may be obtained.

REFERENCES

[Donelan, Hamilton, and Hui, 1985] Donelan M. A., J. Hamilton, and W. H. Hui, "Directional Spectra of Wind-Generated Waves" Philosophical Transactions of the Royal Society of London, vol. 315, no. A, pp. 509-562, 1985.

[Durden and Vesecky, 1985] Durden, S. L. and J. F. Vesecky, "A Physical Radar Cross-Section Model for a Wind-Driven Sea with Swell" IEEE Journal of Oceanic Engineering, vol. 10, no. 4, pp. 445-452, October 1985.

[Gotwols and Thompson, 1994] Gotwols, B. L., and D.R. Thompson, "Ocean Microwave Backscatter Distributions" Journal of Geophysical Research, vol. 99, no. C5, pp. 9741–9750, May 15 1994.

[Phillips, 1985] Phillips, O. M., "Spectral and Statistical Properties of the Equilibrium Range in Wind Generated Gravity Waves" Journal of Fluid Mechanics, vol. 156, pp. 505–531, 1985.

[Plant, 1986] Plant, W. J., "A Two Scale Model of Short Wind-Generated Waves and Scatterometry" IEEE Journal of Geoscience and Remote Sensing, vol. 91, no. 9, pp. 10735–10749, 1986.

[Reed, 1995] Reed, R., "Statistical Properties of the Sea Scattered Radar Return" Dissertation, Brigham Young University, December 1995.

[Sverdrup and Munk, 1947] Sverdrup, H. U., W. H. Munk, "Wind, Sea, and Swell: Theory of Relations for Forecasting" U. S. Navy Hydrographic Office, H. O. Publ., no. 601, 1947.

[Valenzuela and Laing, 1971] Valenzuela, G. R., and M.B. Laing, "On the Statistics of Sea Clutter" Rep. 7349, U.S. Naval Research Lab., Washington D.C., 1971.